Evolved stars with circumstellar shells

Oudmaijer, René Dick

4 Time resolved spectroscopy of the post-AGB star HD 56126 ⋆

Abstract. We have investigated the report of Tamura and Takeuti that the Hα line of the F type post-AGB star HD 56126 is variable on timescales of minutes. To this end, HD 56126 was observed on two occasions with the William Herschel Telescope. Seventeen, respectively thirty spectra were taken within timespans of 1.5 hours in order to detect any short term variations. We find that the Hα line profile changed strongly over the two month interval, but no evidence is found for short term variability. The variability Tamura and Takeuti claim to find is probably due to the low signal-to-noise in their spectra.

1 Introduction

HD 56126 (F5I, $7^h13^m25.3^s$ $+10^o05'09''$) belongs to the class of the so-called high latitude supergiants that are thought to be in the post-Asymptotic Giant Branch (post-AGB) phase of their evolution. These are stars with supergiant spectral types, but are located at unexpectedly high Galactic latitudes. After it was found that most of these stars show far-infrared excess emission due to thermally re-radiating dust (Parthasarathy and Pottasch 1986; Trams et al. 1991; Oudmaijer et al. 1992; Kwok 1993) the post-AGB nature became a widely accepted interpretation for these stars. The infrared excess is explained as being a remnant of the high mass loss the stars underwent during the AGB phase. The evolved status makes the objects less luminous and older compared to massive supergiants, placing them closer to the plane and allowing them more time to get there, solving the high latitude problem.

During the AGB phase, carbon rich material from the helium burning shell was dredged up to the photosphere of HD 56126. This is suggested by the detection of the 3.3 μm infrared 'PAH' feature by Kwok et al. (1990), and the detection of C_2 and CN absorption lines in the optical spectrum by Bakker et al. (1995). A study by Parthasarathy et al. (1992) showed that HD 56126 is metal deficient by a factor of 10 with respect to solar metallicities, although C, N, O, and S appeared solar. This photospheric abundance pattern resembles that of interstellar gas, where the metals have been condensed onto grains (Lambert et al. 1988; Bond, 1991; van Winckel et al. 1992).

⋆ *René Oudmaijer and Eric Bakker, 1994 MNRAS 271, 615*

One of the main problems in the study of late stages of stellar evolution of low to intermediate mass stars is whether there is mass loss during the post-AGB phase, and if there is, the magnitude of the mass loss rate. After the core mass, the post-AGB mass loss rate is the most important parameter governing the time scale of the evolution of these objects from the AGB to the Planetary Nebula (PN) phase. For example the transition of a star with a core mass 0.546 $M_\odot$ having a Reimers mass loss of 10^{-8} $M_\odot yr^{-1}$ takes 100,000 years (Schönberner, 1981; 1983). A period in which the AGB wind has dispersed into the interstellar medium long before the central star has reached a temperature high enough to ionize its circumstellar shell and become observable as a PN. However, as pointed out by Trams et al. (1989), increasing the mass loss rate to 5×10^{-7} $M_\odot$ yr^{-1} accelerates this transition to only 5000 years, which would make a PN readily observable. It is difficult however to determine post-AGB mass loss rates. All 'classic' tracers of mass loss rates such as circumstellar CO millimeter emission, far infrared excesses etc. trace the former AGB wind rather than the present-day mass loss in post-AGB stars.

Most of the post-AGB stars exhibit mild Hα emission. Some objects show strong P Cygni type emission, while most of the stars have shell type profiles. In the recent literature the Hα emission has been interpreted as the star undergoing a post-AGB mass loss (Trams et al., 1989; Parthasarathy et al., 1992; Slijkhuis 1992). In fact, the Hα emission is, next to the near-infrared excess observed in some of the objects (Trams et al., 1989), the only diagnostic suggested for post-AGB mass loss. Although a P Cygni type emission can be understood with a simple expanding wind model, the double peaked shell type profiles require somewhat more complicated geometries as for example rotating disks (Waters et al. 1993). The mass loss interpretation gets more into difficulties when considering the fact that many of the stars show variable Hα profiles. Some of the stars have shell type Hα lines where the ratio between the blue and the red peaks varies on timescales of months (Arellano Ferro, 1985; Waelkens et al. 1991, Waters et al. 1993). Only in the case of HR 4049 the Hα variability could be correlated with radial velocity variations and the orbital phase of the star in a binary system (Waelkens et al. 1991). Although the number of binary stars in the sample of post-AGB stars under consideration is relatively high (Waelkens and Waters, 1993), not all stars that exhibit Hα variations are yet identified as members of a binary system.

Another interpretation that can give rise to variable Hα emission of post-AGB stars stems from stellar pulsation theory. The F-G type post-AGB stars are located in a part of the HR diagram where the photosphere is subject to instabilities (Sasselov 1993; Zalewski 1992). A consequence of such instabilities has been pointed out by Lèbre and Gillet (1991a+b, 1992) in their work on RV Tauri and W Virginis stars, objects that resemble post-AGB stars very closely. These stars show variable Hα emission during their pulsation cycle. Lèbre and Gillet showed that inward and outward moving shocks within the photosphere can produce line profiles remarkably similar to those observed in the post-AGB stars discussed above.

In this work we aim at confirming the rapid changes of the Hα profile of HD 56126 described by Tamura and Takeuti (1993, hereafter TT93). These authors reported Hα line profile variations on timescales of the order of minutes. If the variability on minute time scales is real, it will prove very hard to attribute the observed Hα emission to mass loss. In principle it may be possible to have short 'puffs' of mass ejected from the photosphere and falling back again, giving rise to respectively blue and red emission peaks. Such 'puffs' are then indicative of a turbulent photosphere, so the mass loss and stellar pulsation should be closely intertwined. It would then be more reasonable to explain the rapid Hα variability in terms of pulsation solely than a combination of mass loss and pulsation together. Realizing the important implications caused by the short term variability reported by TT93, we decided to obtain a set of high quality spectra with short exposure times of HD 56126. For this purpose the Utrecht Echelle Spectrograph mounted on the 4.2m WHT telescope on La Palma was employed.

2 Observations and data reduction

2.1 Observations

The first set of observations was carried out on December 21^{st} 1993 in service time with the Utrecht Echelle Spectrograph (Unger, 1994) mounted on the Nasmyth platform of the 4.2 m William Herschel Telescope, La Palma, Spain. The weather was fair, but the seeing was larger than $2''$, which, compared with the slitwidth of $1''$, resulted in a somewhat lower signal-to-noise of the spectra than could have been possible. The detector was a 1124×1124 TEK CCD. Wavelength calibration was performed by observing a Thorium-Argon lamp. The central wavelength of the setting was 5587 Å, resulting in a wavelength coverage from 4700 – 7200 Å. In order to make a compromise between signal-to-noise and time resolution, it was decided to make exposures with increasing integration times.

A second set of data was obtained during a run on the WHT in the night of February 26-27 1994. The settings were the same as for the December run, except for the central wavelength (7127 Å), resulting in a wavelength coverage from 5500 Å – 1 μm. This time the strategy was aimed at searching for time variations within minutes. Thirty exposures of 60 seconds and 30 seconds were taken consecutively. The sky was cloudy, resulting in many telluric features in the spectra. The spectral resolution as measured from telluric absorption lines (full width at half maximum) is 8.5 km s^{-1}. The logs of the observations and the resulting signal-to-noise ratios (measured in the Hα order) are provided in Tables 1 and 2.

2.2 Data reduction

The data were reduced using the standard echelle reduction software in the IRAF package. The data were bias subtracted and divided by a normalized flatfield frame. After the

Table 1 Log of the observations December 21 1993

Time U.T.	T_{exp} s	Airmass	SNR
23:24:39	60	1.465	50
23:27:58	60	1.446	52
23:30:56	90	1.430	62
23:37:41	90	1.394	63
23:41:05	90	1.378	63
23:44:40	180	1.361	87
23:49:35	180	1.339	89
23:54:29	180	1.318	83
23:59:23	180	1.299	82
00:05:25	240	1.276	98
00:11:19	240	1.256	90
00:17:10	240	1.237	99
00:23:09	240	1.219	95
00:29:12	240	1.202	103
00:35:08	240	1.186	100
00:41:11	240	1.171	90
00:47:11	240	1.158	94

The SNR has been calculated in the line free region between 6533 - 6540Å.

flatfielding, the individual orders were optimally extracted from the image frame, where, using simple photon statistics, pixels are weighted.

The spectra contained 44 orders in the December run, and 48 in the February run. The orders were continuum normalized for further analysis. The wavelength calibration was done by fitting a 3^{rd} order Legendre polynomial in the dispersion direction and a 4^{th} order polynomial in the cross-order direction. The dispersion of the fit through the more than 500 identified Th-Ar lines was 3.8 mÅ and 7 mÅ for the December and February spectra respectively. During the process of extraction the signal-to-noise ratio of the pixels was calculated with simple photon statistics. Checks with the actual observed signal-to-noise of the data proved to be correct within 15%. The SNR spectra calculated in this way will be used further in this study.

3 Is there variability?

3.1 Time scales of minutes

In Fig. 1 all individual spectra around Hα obtained December 1993 are plotted. In order to decide whether there are any variations in the spectra we adopt the simple, yet powerful

Table 2 Log of the observations February 27 1994

Time U.T.	T_{exp} s	Airmass	SNR
23:30:35	60	1.133	58
23:34:37	60	1.141	55
23:37:39	60	1.147	53
23:40:39	60	1.153	37
23:43:52	60	1.160	47
00:22:18	60	1.26	72
00:25:39	60	1.280	60
00:28:51	60	1.292	68
00:31:54	60	1.303	55
00:35:23	60	1.317	60
00:38:37	60	1.331	48
00:41:48	60	1.344	55
00:44:58	60	1.359	73
00:47:53	60	1.372	52
00:56:58	60	1.417	64
01:00:10	60	1.435	57
01:03:23	60	1.453	60
01:06:38	60	1.471	58
01:10:06	60	1.492	53
01:13:26	60	1.513	59
01:16:39	60	1.534	50
01:19:57	60	1.557	60
01:23:08	30	1.580	45
01:25:32	30	1.597	29
01:27:57	30	1.616	33
01:30:39	60	1.637	54
01:33:32	60	1.660	63
01:36:26	60	1.685	56
01:39:21	60	1.711	59
01:42:18	60	1.738	53

statistical formalism presented by Fullerton (1990) and Henrichs et al. (1994). With this method the variability can be expressed in a temporal variance spectrum (TVS):

$$(TVS)_\lambda \approx \frac{1}{N-1}\sum_{i=1}^{N}\left(\frac{F_i(\lambda)-F_{av}(\lambda)}{\sigma_i(\lambda)}\right)^2 \quad (1)$$

where N is the number of spectra, $F_{av}(\lambda)$ represents the constructed average spectrum, $F_i(\lambda)$ the individual spectra, and $\sigma_i(\lambda)$ = $F_i(\lambda)$/(SNR) of each individual pixel of the spectra.

Following Henrichs et al. (1994) and Fullerton (1990) the temporal sigma spectrum (TSS = $\sqrt{TVS}$) is calculated. This quantity represents approximately (σ_{obs}/σ_{av}), that is the

standard deviation of the variations of the individual spectra with respect to the average spectrum divided by the standard deviation of the average spectrum. If no significant variations are present in the spectra, the value will be close to one, significant deviations are directly represented in units of the noise level, that is to say a peak 'Temporal Sigma Spectrum' of three corresponds to a variability at a 3σ level.

The individual spectra and the resulting TSS are plotted around Hα in Fig.1. It is clear from the temporal sigma spectrum that no significant variability is present. The spikes in the TSS spectrum correspond to cosmic ray hits that resulted in higher count levels and consequently higher signal-to-noise ratios. These cosmic ray events are still a bit present in the spectra, and provide an independent check whether the method is indeed capable of detecting variability. Another way to demonstrate the adequacy of the method can be found in Fig. 2, where we have plotted the first and last taken spectrum around 6875 Å during the December run. The effect of the decreasing airmass on the strength of telluric absorption lines is seen.

The same procedure was carried out for the February observations. The average spectrum and the resulting TSS are shown in Fig. 3. No variability can be found either in the February run. The shallow shape of the TSS arises from the fact that the normalization of the spectrum was difficult, leading to a small variation of the continuum in the wings of the Hα line.

Similar calculations were performed for spectra with the same integration times, and for the rest of the UES spectrum. Except for strong telluric absorption lines (see Fig. 2) no variations are present.

3.2 Time scales of months

Average spectra were computed by adding all spectra before the continuum correction, resulting in spectra with a high SNR (> 300 and > 175 respectively for the December and February observations). The radial velocity is not significantly variable, the heliocentric velocity we derive from strong metallic lines are 87 ± 2 km s^{-1}, and 84 ± 2 km s^{-1} for the December and February spectra respectively.

In Fig. 4 the Hα lines at both occasions are shown. The profiles are markedly different; whereas in the December spectrum the Hα profile shows a central absorption at 103 km s^{-1}, it has shifted to 94 km s^{-1} in February, the peaks around the Hα absorption have increased in strength. The true shape of the emission is hard to determine, but considering the red-shifted center of the Hα absorption, there appears to be a rather broad emission component blueshifted by more than 20 km s^{-1}.

Not only the Hα lines differ, a preliminary comparison of the individual spectra shows that all spectral lines are broader by more than 40% at their full width half maximum, while the depression relative to the continuum decreased in the February spectra relative to the December spectrum. Interestingly, except for the strongest metallic lines (depression < 50 %) where a blueshifted absorption wing is visible, all lines appear symmetric. The interstellar component in the profiles of the NaI D1 & D2 lines do not change in velocity

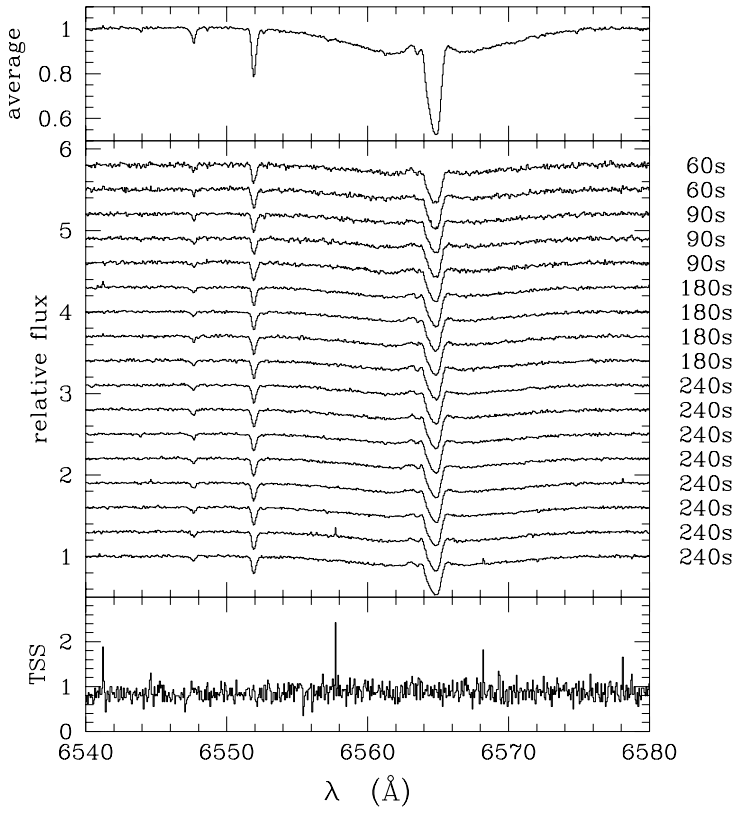

Figure 1 *The 17 spectra that were obtained around Hα during the December run. The spectra are continuum normalized, each spectrum is plotted with an offset of 0.3 for comparison. The Temporal Sigma Spectrum (see text for details) is also plotted. Note that the small spikes in the individual spectra are immediately visible in the TSS.*

nor in shape between the two spectra, indicating that changes in other lines are not due to observational errors. For the FeI and FeII lines we note that the equivalent width of the FeI lines decreased, while the equivalent width of the FeII lines has increased. The fact that the ionization degree of Fe has changed indicates an increase of the effective temperature, the broader lines are probably the result of a higher surface gravity. The deeper central absorption in the Hα line is also due to an increase of the effective temperature which gives a higher population of the n=2 level for hydrogen according to the Boltzmann law.

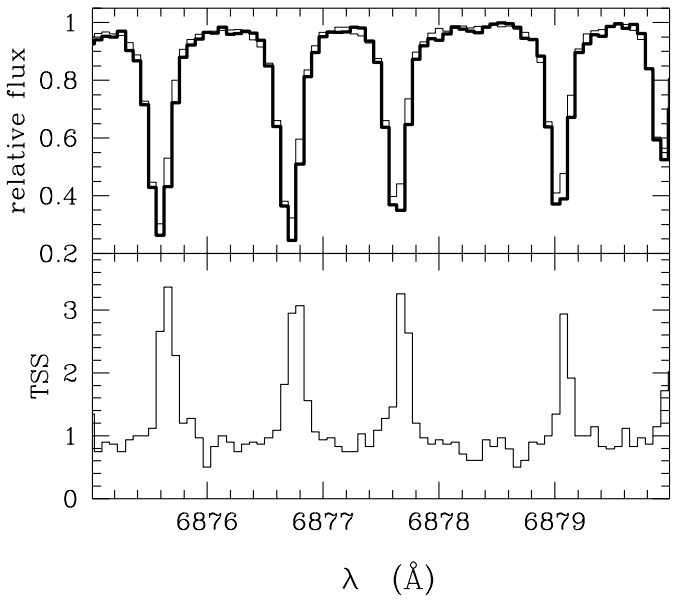

Figure 2 *An overplot of the first spectrum (thick line, airmass 1.47) and the last spectrum (thin line, airmass 1.16) taken around 6875Å in December is shown in the upper panel. The lower panel shows the Temporal Sigma Spectrum. It can be seen that the variable telluric absorption lines show up as significant peaks in the TSS.*

4 Discussion

In section 3.1 it was shown that no short term variability is found in the Hα line of HD 56126. Before we discuss any explanation for this observational result, let us first review the data presented by TT93. They presented 5 spectra of HD 56126 taken with the 74 inch Okayama telescope. The spectra were obtained within 47 minutes, with 6 minutes the shortest time interval between two observations. The wavelength resolution is about 0.13 Å (6 km s^{-1} at Hα), comparable to the spectra presented here. From their plots we find for their best spectrum a peak-to-peak noise of approximately 17% of the continuum level and of about 30% for the other spectra. We estimate their SNR at about 10-20. Of the 5 spectra 3 show an absorption profile, only two show the variation noticed by TT93. One of these shows a red emission peak at while another spectrum shows a blue peak, which they claim to be "drastic changes of the Hα profile in the order of ten minutes". In fact, these are the only spectra that show noticeable variations. The signal-to-noise of their spectra is at most 20, so that a 1σ variation has to be at least a 5% change for an unresolved line.

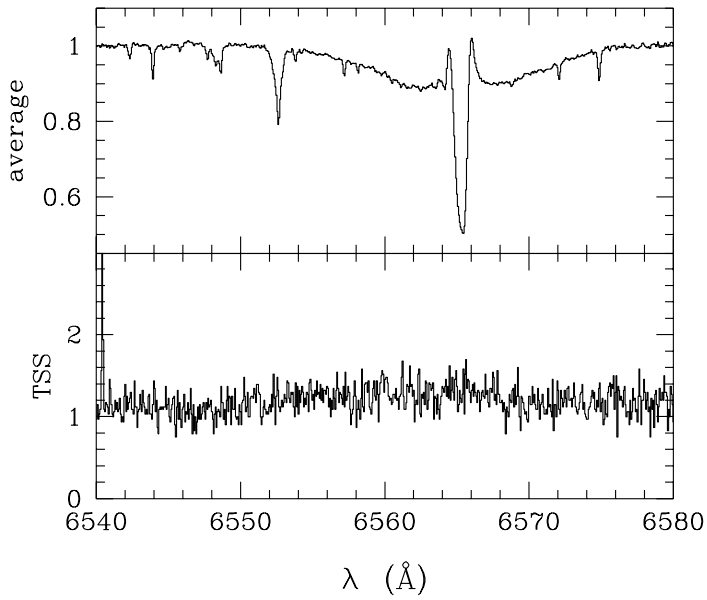

Figure 3 *The summed spectrum and the resultant Temporal Sigma Spectrum of the observations obtained in February 1994. The slight curvature of the TSS arises from the fact that the normalization of the spectrum was difficult, leading to small variations of the continuum in the wings of the Hα line.*

The (variable) emission components hardly exceed this value. Furthermore, the strong SrI line at 6550.2 Å (E.W. = 77 mÅ, depression to 0.8 $\times$ continuum) is present in only 2 of their spectra. This further suggests that the observed changes may be artifacts of the noise rather than true changes in the spectrum.

In section 3.2 it was argued that, due to the broadening of most stellar lines and the change in ionization degree of Fe, the star has become hotter over a time interval of 65 days. This indicates that the star is variable, consistent with the findings of Bogaert (1994), who found photometric variability of HD 56126. It is still hard to identify the mechanism responsible for the emission observed in Hα. It can be due to mass loss, where the stronger emission in the February spectrum is simply due to the increased temperature of the star, it could also be due to a shock wave ploughing through the photosphere. It may be worthwhile to monitor post-AGB stars on timescales of days and weeks to appreciate the true temporal changes in their spectra.

Finally we consider whether the absence of any short term variability can be expected based on simple arguments; in principle the fastest timescale in which a wave can propa-

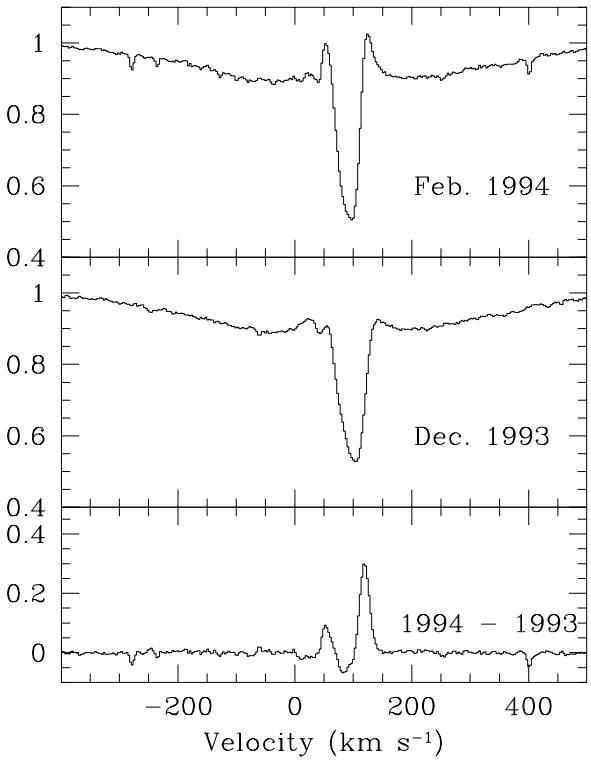

Figure 4 *Hα profiles of HD 56126 at the two epochs. The difference spectrum is shown in the lower panel.*

gate in a stellar atmosphere is the scaleheight h divided by the speed of sound v_s:

$h = \frac{kTR^2}{\mu m_H MG}$ m

$v_s \sim \sqrt{\frac{kT}{\mu m_H}}$ km s^{-1}

With M the mass of the star and R its radius, μ is the mean molecular weight which is taken to be 1. Adopting typical parameters for an F type post-AGB star, M = 0.6 $M_\odot$, and R = 60 $R_\odot$, we obtain a shortest possible timescale of 1.8 days.

One can also estimate the pulsation period of a typical post-AGB star:

$$\tau_P = \mathrm{Q} \times \sqrt{\left(\frac{R_*}{R_\odot}\right)^3 \left(\frac{M_\odot}{M_*}\right)} \quad \text{days}$$

Where Q is the pulsation constant in days. Adopting the same stellar parameters as above, and noting that Q ranges from 0.04 for classical Cepheids to 0.16 for W Virginis stars (Allen, 1973) we obtain an expected period of 30 – 96 days. This simple exercise tells us that variations on timescales shorter than days are not really to be expected in post-AGB stars. It is consistent with the change observed over a period of two months.

5 Conclusions

We observed the post-AGB star HD 56126 (F5I) at short intervals in order to look for very short term variations of the Hα line. Despite the high quality of the data we were not able to find significant variations. The report by Tamura and Takeuti (1993) that the line is variable within minutes could not be confirmed. We believe that the variability they claim is due to the low signal-to-noise of their spectra and not due to real variability. Strong variations are found over the two month interval, where the central absorption of the Hα line has shifted and both peaks around the central absorption have increased considerably. It is shown that the star has increased its surface temperature over two months, indicating that the underlying star rather than the circumstellar environment changes, adding more validity to pulsational models that account for observed changes in spectra of post-AGB stars.

Acknowledgements We wish to express our gratitude to René Rutten for carrying out the service observations. Ton Schoenmaker is greatly acknowledged for introducing RDO to the IRAF reduction software package. We enjoyed the enlightening discussions with Peter van Hoof, Rens Waters, Henny Lamers and Norman Trams. Griet Van de Steene is acknowledged for her comments on an earlier version of the manuscript. Finally we wish to thank the referee, Christoffel Waelkens for his constructive remarks. RDO and EJB receive financial support under grants no. 782-372-031 and 782-371-040 from the Netherlands Foundation for Research in Astronomy (ASTRON) which receives its funds from the Netherlands Organisation for Scientific Research (NWO). The William Herschel Telescope is operated on the island of La Palma by the Royal Greenwich Observatory in the Spanish Observatorio del Roque de los Muchachos of the Instituto de Astrofísica de Canarias.

References

Allen C.W. 1973, "Astrophysical Quantities", The Athlone Press, London, p.217

Arellano Ferro A. 1985, Rev. Mex. Astr. Astr. 11, 113

Bakker E.J., PhD Thesis, University of Utrecht

Bakker E.J., Waters L.B.F.M., Lamers H.J.G.L.M., Trams N.R., van der Wolf F.L.A. 1995, A&A in press

Bogaert E. 1994, PhD thesis, University of Leuven
Bond H.E. 1991, in "Evolution of stars: the photospheric abundance connection", eds. Michaud G. and Tutukov A., Kluwer, Dordrecht, p.341
Fullerton A.W. 1990, PhD thesis, University of Toronto
Henrichs H., Kaper L., Nichols J.S. 1994, A&A 285, 565
Kwok S., Hrivnak B.J., Geballe T.R. 1990, ApJ 360, L23
Kwok S. 1993, ARAA 31, 63
Lambert D.L., Hinkle K.H., Luck R.E. 1988, ApJ 333, 917
Lèbre A. and Gillet D. 1991a, A&A 246, 490
Lèbre A. and Gillet D. 1991b, A&A 251, 549
Lèbre A. and Gillet D. 1992, A&A 255, 221
Oudmaijer R.D., Van der Veen W.E.C.J., Waters L.B.F.M., Trams N.R., Waelkens C., Engelsman E. 1992, A&AS 96, 625 (Chapter 2)
Parthasarathy M. and Pottasch S.R. 1986, A&A 154, L16
Parthasarathy M., Garcia Lario P., Pottasch S.R. 1992, A&A 264, 159
Sasselov D.D. 1993, in "IAU Symposium No. 155 Planetary Nebulae" eds. Weinberger R. and Acker A., Kluwer academic publishers, The Netherlands, p.249
Schönberner D. 1981, A&A 103, 119
Schönberner D. 1983, ApJ 272, 708
Slijkhuis S. 1992, Ph.D. thesis University of Amsterdam, The Netherlands
Tamura S. and Takeuti M. 1993, in "Luminous high latitude stars", ed. Sasselov S.S., Astronomical society of the Pacific conference series Vol. 45, ASP, USA, p.309 (TT93)
Trams N.R., Waters L.B.F.M., Waelkens C., Lamers H.J.G.L.M., Van der Veen W.E.C.J. 1989, A&A 218, L1
Trams N.R., Waters L.B.F.M., Lamers H.J.G.L.M., Waelkens C., Geballe T.R., Thé P.S. 1991, A&AS 87, 361
Unger S. 1994, La Palma Technical Notes no. XXIII
Van Winckel H., Mathis J.S., Waelkens C. 1992, Nat. 356, 500
Waelkens C., Lamers H.J.G.L.M., Waters L.B.F.M., Rufener F., Trams N.R., Le Bertre T., Ferlet R., Vidal-Madjar A. 1991, A&A 242, 433
Waelkens C. and Waters L.B.F.M. 1993, in "Luminous high latitude stars", ed. Sasselov S.S., Astronomical society of the Pacific conference series Vol. 45, ASP, USA, p.219
Waters L.B.F.M, Waelkens C., Trams N.R. 1993, in "Second ESO/CTIO workshop Mass loss on the AGB and beyond", ed. Schwarz H.E., ESO Conference and Workshop Proceedings No. 46, Germany, p.298
Zalewski J. 1992, PASJ 44, 27